Recognition of Cisplatin−DNA Interstrand Cross-Links by Replication Protein A[†]

Steve M. Patrick,*[,‡] Kristin Tillison,[‡] and Jeffrey M. Horn[§]

Department of Biochemistry and Cancer Biology, University of Toledo Health Science Campus, Toledo, Ohio 43614, and Wright State University Nursing Program, Dayton, Ohio 45435

Received March 18, 2008; Revised Manuscript Received July 30, 2008

ABSTRACT: Replication protein A (RPA) is a heterotrimeric protein that is required for DNA replication and most DNA repair pathways. RPA has previously been shown to play a role in recognizing and binding damaged DNA during nucleotide excision repair (NER). RPA has also been suggested to play a role in psoralen DNA interstrand cross-link (ICL) repair, but a clear biochemical activity has yet to be identified in the ICL DNA repair pathways. Using HeLa cell extracts and DNA affinity chromatography, we demonstrate that RPA is preferentially retained on a cisplatin interstrand cross-link (ICL) DNA column compared with undamaged DNA. The retention of RPA on cisplatin intrastrand and ICL containing DNA affinity columns is comparable. *In vitro* electrophoretic mobility shift assays (EMSAs) using synthetic DNA substrates and purified RPA demonstrate higher affinity for cisplatin ICL DNA binding compared with undamaged DNA. The enhanced binding of RPA to the cisplatin ICL is dependent on the DNA length. As the DNA flanking the cisplatin ICL is increased from 7 to 21 bases, preferential RPA binding is observed. Fluorescence anisotropy reveals greater than 200-fold higher affinity to a cisplatin ICL containing 42-mer DNA compared with an undamaged DNA and a 3−4-fold higher affinity when compared with a cisplatin intrastrand damaged DNA. As the DNA length and stringency of the binding reaction increase, greater preferential binding of RPA to cisplatin ICL DNA is observed. These data are consistent with a role for RPA in the initial recognition and initiation of cisplatin ICL DNA repair.

Replication protein A, RPA,[1] was first identified as a DNA replication factor (*1*). It is a heterotrimeric protein consisting of 70 (RPA1), 32 (RPA2) and 14 (RPA3) kDa subunits (*2*). RPA displays a high affinity for single-stranded DNA (ssDNA) and is responsible for stimulating helicase DNA displacement activity and maintaining ssDNA during DNA replication (*3*). RPA also plays a role in stimulating polymerase α activity (*4*). It has since been shown to be required for nucleotide excision repair (NER), mismatch repair (MMR) and homologous recombination (HR) (*5*−*7*). The central role of RPA in these DNA repair pathways is to bind DNA and help recruit and position processing enzymes (*8*). It is through the protein−protein interactions that RPA can regulate the metabolic processes that occur within the cell (*9*). In NER, RPA is believed to play a role in DNA damage recognition and helps position the endonucleases XPG and XPF-ERCC1 to the 3′ and 5′ sides of the damaged DNA, respectively (*10*−*12*).

RPA consists of oligonucleotide/oligosaccharide binding (OB)-folds within the subunits that form a groove around ssDNA and have been termed DNA binding domains (DBDs) (*13*). There are currently six DBDs located within the heterotrimer. DBD A and B are located in the central region of the 70 kDa subunit, while DBD C is located at the C-terminus of the 70 kDa subunit (*13*−*15*). DBD F resides in the N-terminal domain of RPA 70 (*16*). DBD D is located within the central region of the 32 kDa subunit and has weak DNA binding activity (*17*). The 14 kDa subunit is composed of an OB-fold that has been defined as DBD E and appears critical for heterotrimeric formation, but it is still unclear if it interacts with DNA (*17*).

RPA binds to ssDNA in a distinct polarity (*12*). The DBDs A and B of the 70 kDa subunit bind to the 5′ side of the DNA followed by DBDs C and D binding and extending along the DNA in the 3′ direction (*13, 18*). *In vitro* binding characterization of RPA has demonstrated a higher affinity for bulky DNA damage compared with undamaged DNAs (*19*). The binding mechanism relies on RPA's ability to recognize the structural distortion in DNA generated by bulky damage and subsequently binding and denaturing the duplex damaged DNA (*20, 21*). During NER, RPA binds to the undamaged DNA strand to help direct incision to the damaged DNA strand (*12, 21*). This binding mechanism protects the undamaged DNA strand and helps position the XPG and XPF-ERCC1 endonucleases to cleave the damaged DNA strand at their respective 3′ and 5′ positions to the adduct (*12*).

Interstrand cross-links (ICLs), including those generated by the chemotherapeutic drug cisplatin, are a complex lesion

[†] This work was supported by a research grant from the American Cancer Society (ACS, RSG-06-163-01-GMC) to S.M.P.

* To whom correspondence should be addressed: Department of Biochemistry and Cancer Biology, 3035 Arlington Ave., University of Toledo Health Science Campus, Toledo, OH 43614. Tel: (419)383-4152. Fax: (419)383-6228. E-mail: Stephan.Patrick@utoledo.edu.

[‡] University of Toledo Health Science Campus.

[§] Wright State University Nursing Program.

[1] Abbreviations: RPA, replication protein A; ssDNA, single-stranded DNA; NER, nucleotide excision repair; MMR, mismatch repair; HR, homologous recombination; ICLs, interstrand cross-links; bp, base pairs; kDa, kilodalton; OB, oligosaccharide/oligonucleotide binding; B-DNA, biotinylated DNA; DBDs, DNA binding domains; TCA, trichloroacetic acid; EMSA, electrophoretic mobility shift assay; DSB, double strand break; ND, not determined; K_D, dissociation constant.

10.1021/bi800460d CCC: $40.75
Published on Web 08/26/2008

that covalently links duplex DNA molecules. Cisplatin forms both intrastrand (intra) and ICL DNA adducts (*22*). The cisplatin ICLs are a low abundant lesion, but one that is believed to play a significant role in the cytotoxic efficacy of the drug. Due to the covalent link between the duplex DNA structure, the ICLs are an absolute block to the DNA replication and transcription machinery. It appears that cells use multiple mechanisms to repair ICL damaged DNA, including NER, HR and lesion bypass mechanisms (*23, 24*). These pathways can be error free or error prone in nature (*23, 25*). The exact mechanisms and biochemical events that occur during ICL DNA repair remain poorly understood.

RPA has been suggested to play an early role in psoralen ICL repair (*26*). Considering the duplex denaturing mechanism that RPA utilizes for bulky DNA adduct binding, it is unclear what role RPA plays other than polymerase stimulation following a dual incision mechanism in psoralen ICL repair (*26*). There is evidence that RPA and the xeroderma pigmentosum group A (XPA) protein can bind and recognize triplex DNAs containing a psoralen ICL (*27*). Whether this binding is due to the triplex structure or the DNA structure generated by the psoralen ICL remains to be determined. Also, using small duplex DNA substrates 19 bases in length, we have previously shown that a cisplatin ICL inhibits DNA binding in an electorphoretic mobility shift assay (EMSA) (*28*).

To date, a clear biochemical role for RPA in ICL repair has yet to be determined. In this report, we provide evidence that RPA can bind to a cisplatin ICL damaged DNA using DNA affinity chromatography. Using purified proteins and synthetic DNA substrates, we demonstrate that RPA displays a significantly higher affinity for a cisplatin ICL damaged DNA compared with undamaged DNA and a moderately higher affinity compared with intrastrand GXG DNA. The preferential RPA binding to the cisplatin ICL is DNA length dependent, which suggests that RPA is binding to the structural distortion that flanks the ICL. This data is consistent with RPA playing a role in the recognition of cisplatin ICL DNA and likely plays a role in the initiation of cisplatin ICL repair and recruitment of DNA processing enzymes.

MATERIALS AND METHODS

Materials. DNA oligonucleotides were purchased from IDT DNA Technologies (IDT), Inc. (Coralville, IA). T4 polynucleotide kinase and mung bean nuclease and restriction endonucleases were from New England Biolabs (Beverly, MA). Radiolabeled nucleotides were from PerkinElmer Life Sciences (Boston, MA). The monoclonal RPAp32 antibody (RPA/p34 Ab-1), the monoclonal XPA antibody (XPA Ab-1) and the monoclonal Ku 80 antibody (Ku Ab-2) were from Neomarkers (Fremont, CA). Cyanogen bromide (CNBr) activated Sepharose 4B was from Amersham Biosciences/GE Healthcare (Piscataway, NJ). The streptavidin-magnetic beads were from Promega (Madison, WI). All other reagents and chemicals were from standard suppliers.

Protein Purification. Recombinant human RPA was purified as previously described using the expression vector kindly provided by Marc Wold (*19*−*21*). Active RPA was determined for each separate protein preparation and normalized in the reactions. This was achieved by performing stoichiometric binding using F-dT30 ssDNA in anisotropy assays similar to that previously described (*29*).

Table 1: DNA Substrates

DNA	sequence (5′-3′)[a]
15GXG	TTCTT**GCG**CTTCTTT
15ICL	TTCTTCT**G**CTTCTTT
42GXG	CTCTTCCCCCTCTCCTTCTT**GCG**C TCTTCCTTCCCCTTCCCT
42ICL	CTCTTCCCCCTCTCCTTCTT**G**CCC TCTTCCTTCCCCTTCCCT
60GXG	CCCTTCTTTCTCTTCCCCCTCTCC TTCTT**GCG**CTCTTCCTTCCCCTTCCCTTTCCTCCCC
60ICL	CCCTTCTTTCTCTTCCCCCTCTCC TTCTT**G**CCCTCTTCCTTCCCCTTCCCTTTCCTCCCC

[a] The oligos were annealed to complementary DNA strands to generate duplex DNA substrates. The position of the cisplatin adduct is shown in bold, and the *Hha*I site is underlined.

Synthetic DNA Purification. DNA substrates were designed to contain a centrally located cisplatin intrastrand 1,3dGXG DNA adduct or a cisplatin ICL (Table 1). The DNA substrates were either left untreated (undamaged DNA) or treated with cisplatin to induce adduct formation. Following platination, the unreacted cisplatin was removed by Qiagen resin and then DNA was ethanol precipitated and subsequently annealed to complementary DNA oligos (*20, 21*). The 1,3dGXG DNA substrate was treated with the restriction enzyme *Hha*I to cleave the undamaged DNA present in the sample to ensure 100% platination (*28*). The undamaged and GXG DNA substrates were then native gel purified to remove ssDNA and cleaved products for the GXG substrates as previously described (*20, 21*). The ICL DNA was incubated at 37 °C for 12−15 h in the presence of 0.05 M $NaClO_4$ and 10 mM Tris pH 7.5 to enable ICL formation (*28, 30*). This process is approximately 10% efficient for generating an ICL containing DNA. The DNA was subsequently ethanol precipitated and purified on a preparative DNA denaturing gel to separate cross-linked and un-cross-linked DNA molecules (*28*). This preparative sequencing gel purification process results in greater than 95% pure cisplatin ICL containing DNA.

Biotin DNA Pull-Downs. Biotinylated (B) 42-mers, either undamaged (-Pt), intrastrand or containing a single ICL DNA adduct, were bound to streptavidin coated magnetic beads (100 pmol each). Initially, the beads were washed with 500 μL of buffer A low salt (100 mM NaCl) three to four times to remove any unbound DNA substrate. Next, equivalent total protein (5−10 μg) of sample from the calf thymus ICL DNA affinity column pools were added to each tube (Supporting Information). This ensured that all B-DNA samples had the same input protein. The tubes were then gently rotated for one hour at 4 °C. The tubes were then placed in a magnetic separation stand which sequesters the beads to a single side of the tube, allowing efficient removal of unbound proteins. The supernatants were then removed and the tubes were washed three times using buffer A low salt. After washing, 250 μL of buffer A high salt (1 M NaCl) was added to each tube and the tubes were rotated for 30 min at 4 °C. The supernatant containing eluted proteins was then collected from each tube and then TCA precipitated using 10% final concentration. The resulting pellets were then resuspended in buffer A low salt and separated by SDS−PAGE, trans-

ferred to PVDF membrane and probed with RPA p32 antibody and a XPA monoclonal antibody.

EMSA Analysis of RPA Binding Synthetic DNAs. 50 fmol of 5′-P^{32} labeled duplex DNA substrates either undamaged, containing a single 1,3d(GXG) intrastrand adduct, or containing a centrally located cisplatin ICL were placed into 20 μL reactions containing 20 mM HEPES, pH 7.8, 2 mM DTT, 0.001% NP-40, 100 mM NaCl, and 2 mM $MgCl_2$. Purified recombinant RPA was titrated where indicated and incubated at room temperature for 15 min. When RPAp32 antibody was used, incubation was carried out for 10 additional minutes at room temperature. The addition of the p32 antibody stabilizes RPA-DNA for better quantification in EMSAs. Reactions were stopped with the addition of gel loading buffer and separated on 4% native polyacrylamide gels. The gels were then dried, exposed to film by autoradiography and quantified by PhosphorImager analysis. The results are the average of at least three independent experiments for all duplex DNA lengths.

Anisotropy Assays. Fluorescein (F) labeled synthetic DNAs either undamaged or containing a centrally located intrastrand or interstrand cross-link were placed in 150 or 25 μL reactions in the presence of increasing concentrations of RPA. Excitation and emission wavelengths were 470 and 525 nm, respectively. Measurements were performed with a Molecular Devices Spectramax M5 fluorescence plate reader using Greiner 96 well or 384 well small volume black plates. The DNA concentration was 1 nM or 5 nM in all reactions. The addition of purified RPA to fluorescein labeled DNA resulted in an increase in the anisotropy value with minimal change in fluorescence intensity as previously seen (*29, 31*). Anisotropy (r) values were calculated from the following equation:

$$r = \frac{I_{VV} - GI_{VH}}{I_{VV} + 2GI_{VH}}$$

where I_{VV} is the parallel component and I_{VH} the perpendicular component of the fluorescence intensity. G is a correction factor for differences in vertically and horizontally polarized light. Measurements were performed in the EMSA buffer with the NaCl and $MgCl_2$ concentrations indicated in the figure legends and Table 2. The results presented are the average of six to nine individual readings. The DNA concentrations were kept much lower than the calculated K_Ds. The graphs were plotted using Sigma Plot 10.0 and fitted to a hyperbolic curve for a simple one site binding mechanism similar to previously published data (*29, 31*). The K_D values are presented in Table 2.

RESULTS

Using DNA affinity chromatography, we have determined that RPA has binding preference for cisplatin ICLs compared with undamaged DNA. See Supporting Information paragraph for details. To further address the affinity of RPA for undamaged, cisplatin intra and cisplatin ICL DNA, site-specific DNA substrates were utilized.

Binding of RPA to Site-Specific Cisplatin ICL DNA. The retention of RPA on the cisplatin ICL column could be due to intra specific lesions that remain on the calf thymus DNA following high levels of cisplatin treatment and incomplete NaCN treatment (see Supporting Information). To confirm

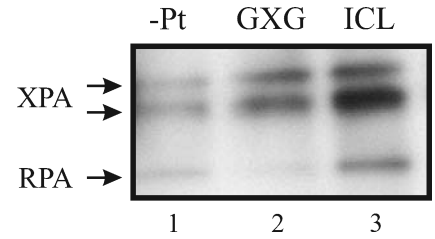

FIGURE 1: RPA binds DNA with a site-specific cisplatin ICL. Duplex biotinylated 42-mers, either left undamaged (-Pt) or containing a single cisplatin GXG or cisplatin ICL, were complexed to streptavidin coated magnetic beads. Equivalent quantities (5−10 μg) of protein eluted from the large scale cisplatin ICL sepharose column were incubated with each of the biotinylated substrates. Using a magnet to sequester the complexes (beads, oligos, and bound proteins), the complexes were washed with low salt buffer and then eluted using high salt buffer with 1 M NaCl. Eluted proteins were then TCA precipitated and loaded onto a SDS gel. The gel was transferred to PVDF membrane for Western blot and probed with antibodies against XPA and RPA as indicated. Lane 1 represents protein bound to the undamaged (-Pt) substrate, lane 2 is the protein bound to the GXG and lane 3 is the protein bound to the cisplatin ICL.

that RPA was binding directly to the cisplatin ICL damaged DNA, synthetic DNA substrates with a centrally located cisplatin ICL were constructed as described in the Materials and Methods section. The DNA substrates (duplex undamaged, intra GXG and ICL 42-mers) contained a 5′-biotin label to use in pull-down experiments with streptavidin magnetic particles. Equal total protein from the calf thymus ICL DNA affinity column (Supporting Information) was reacted with each DNA substrate followed by extensive washing and elution with high salt buffer. The bound protein was TCA precipitated and loaded onto SDS gels. The resulting gels were transferred for Western blot analysis using RPA p32 and XPA monoclonal antibodies (Figure 1). The results indicate that RPA as well as XPA preferentially bind the cisplatin ICL DNA compared with undamaged and intra containing DNA substrates (lane 3 compared with lanes 1 and 2, respectively). The presence of other proteins within this partially purified protein pool could alter the binding of RPA to the DNA substrates or compete with the binding to the damaged DNA. This is one possibility for the lower retention of RPA on the intra DNA compared with undamaged DNA (lane 2 compared with lane 1). XPA and XPF-ERCC1 consistently display preferential binding to the cisplatin ICL, but binding appears to be dependent on RPA (manuscript in preparation). Also, the binding of the global initiator of NER, XPC-hHR23B, showed minimal difference between undamaged, intra and ICL DNA in the large scale calf thymus DNA columns and was used as a loading control between columns (data not shown). *In vitro* binding reactions using purified XPC-hHR23B also demonstrate a lower affinity than RPA for cisplatin ICL DNA (manuscript in preparation).

EMSA Analysis of RPA Binding to Cisplatin ICL DNA. Besides a direct binding mechanism of RPA to cisplatin ICL DNA, another possibility is that a protein−protein interaction within the partially purified pool could enhance RPA retention on the ICL DNA. To address these possibilities and to assess direct RPA-ICL DNA binding, purified recombinant human RPA was incubated with radiolabeled DNA substrates in electrophoretic mobility shift assays (EMSAs). In Figure 2, increasing amounts of RPA were

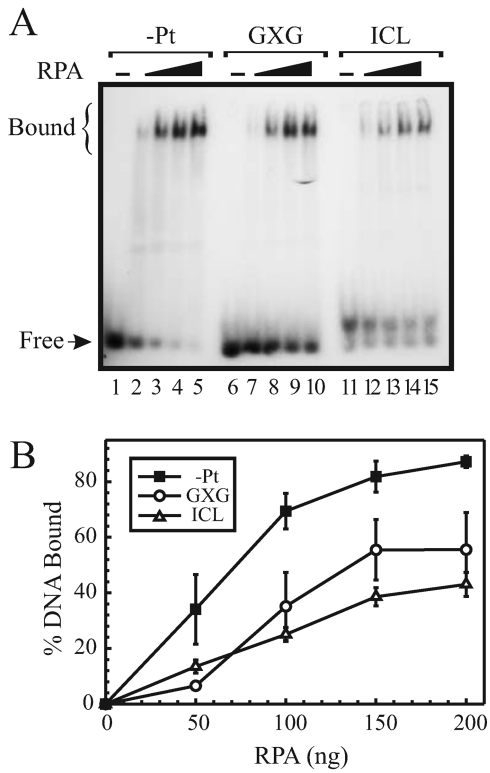

FIGURE 2: Purified RPA binds weakly to cisplatin ICL damaged 15-mer DNA substrates using EMSA. In A, 50 fmol of duplex 15-mer DNA substrate either undamaged (-Pt), intra (GXG) or ICL was incubated with increasing amounts of RPA. The reactions contained 100 mM NaCl and 2 mM $MgCl_2$. Samples were electrophoresed on 4% native gels and visualized by autoradiography. Lanes 1, 6 and 11, no protein; lanes 2, 7 and 12, 50 ng RPA; lanes 3, 8 and 13, 100 ng RPA; lanes 4, 9 and 14, 150 ng RPA; and lanes 5, 10 and 15, 200 ng RPA. In B, quantification of RPA binding to undamaged (squares), intra GXG (open circles) and ICL (open triangles) DNA substrates was determined by PhosphorImager analysis. The results are the average of 3 individual experiments, and the error bars represent the standard deviation.

incubated with radiolabeled duplex 15-mer DNAs (undamaged, intra GXG and ICL) and protein binding was quantified. The RPA p32 antibody was included in the reactions following DNA binding to stabilize the protein−DNA interaction. The addition of the antibody results in less DNA substrate smearing and better RPA binding quantification in the EMSAs (*31*). Increasing RPA protein results in an increase in protein−DNA binding in the undamaged and intra (GXG) DNA substrates, but RPA binding to the ICL DNA is weaker (Figure 2B). In the absence of the p32 antibody, the RPA−ICL DNA binding is further reduced (data not shown). This result is consistent with previous reports that a cisplatin ICL inhibits RPA binding on short duplex DNA substrates using EMSAs (*28*). It is also consistent with the duplex DNA binding mechanism proposed for RPA in which RPA binds a structural distortion induced by bulky DNA damage and subsequently denatures the DNA to bind ssDNA (*20*). The results from the EMSA using the 15-mer ICL DNA, however, are not consistent with the data presented in Figure 1 (as well as Figure S1) where RPA retention is greatest in the cisplatin ICL columns. These discrepancies appear to involve the length of the DNA used, the type, and the sensitivity of the assays used to detect DNA binding. EMSAs are more qualitative in nature and are not typically used for quantifying actual protein affinities for DNA. To

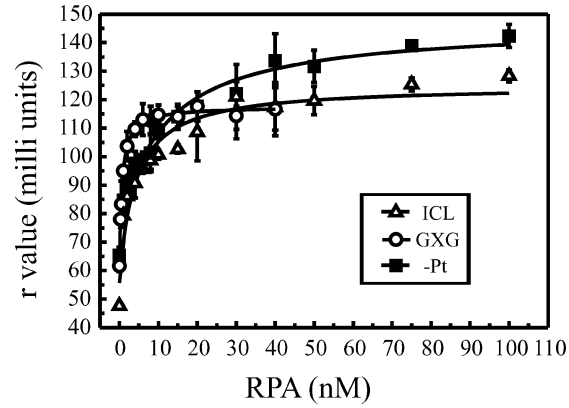

FIGURE 3: Anisotropy reveals binding of RPA to a duplex 15-mer ICL containing DNA. DNA binding of RPA to 15-mer DNA substrates was conducted by anisotropy experiments using fluorescein labeled DNA. Increasing concentrations of RPA (0−100 nM) were added to reactions containing 1 nM duplex undamaged (squares), cisplatin intra GXG (open circles) or cisplatin ICL (open triangles) DNA. The plots were fitted using SigmaPlot and a simple one site protein binding mechanism to determine the K_D of RPA for each DNA substrate. Each point represents 3−6 individual experiments and the error bars represent the standard deviation.

further address whether RPA was binding directly to the cisplatin ICL DNA, a more sensitive assay was utilized.

Binding of RPA to Cisplatin ICL DNA Using Anisotropy. To address RPA binding in a more sensitive solution based assay and to quantify the affinity of RPA for the DNA substrates, fluorescence polarization was utilized (*29, 31*). Fluorescein (F) labeled DNA substrates were generated that were identical in sequence to the DNA substrates used in the EMSAs, and binding reactions were similar to those used in the EMSAs. The rotation of F-DNA substrates is changed upon protein binding and can be monitored by anisotropy (*r* value) using the equation presented in the Materials and Methods section. The change in *r* value with increasing RPA is directly proportional to the amount of RPA bound to DNA (*29, 31*). When the DNA concentration (1 nM for 15-mers) is kept below the estimated dissociation constant (K_D) for RPA binding and RPA protein is titrated into the reaction, a hyperbolic curve results. Fitting the plot to a simple one site binding mechanism yields K_Ds for RPA binding the various DNA substrates (*31*). Using this approach, we have determined the K_D of RPA for duplex undamaged, intra and ICL containing 15-mer DNA substrates in the presence of 200 mM NaCl (Figure 3). The graph results in a K_D of 11.2 nM for undamaged DNA, 0.7 nM for intra DNA and 4 nM for ICL DNA. The K_Ds for all DNA substrates are presented in Table 2. Under less stringent (lower salt) conditions, RPA binds and denatures the duplex 15-mer DNAs similarly and has lower K_D values (data not shown). For the intra DNA, it is difficult to keep the DNA concentration below the K_D value due to instrument sensitivity issues and, thus, this value is only an estimation of the RPA affinity. The results are consistent with RPA having a higher affinity for cisplatin intra damaged DNA (*19*), but also suggest that, in a more sensitive assay, RPA displays preference for the ICL compared with undamaged DNA. Based on RPA's duplex DNA binding/denaturing mechanism, RPA could likely bind the distorted DNA that flanks the ICL. In EMSAs, RPA has low binding levels to DNA substrates shorter than 12 bases and binding is not very stable through the gel

Table 2: K_D Values for RPA Binding DNA[a]

DNA substrate	K_D (nM)
duplex 15-mer -Pt	11.2 ± 2.8
duplex 15-mer GXG	0.7 ± 0.06
duplex 15-mer ICL	4 ± 1.2
duplex 42-mer -Pt	1826 ± 621
duplex 42-mer GXG	36 ± 6.4
duplex 42-mer GXG[b]	81.7 ± 11.1
duplex 42-mer ICL	8.4 ± 2.5
duplex 42-mer ICL[b]	13.8 ± 1.4
duplex 60-mer -Pt	1390 ± 346
duplex 60-mer -Pt[b]	ND[c]
duplex 60-mer GXG	27.1 ± 2.5
duplex 60-mer GXG[b]	1237 ± 119
duplex 60-mer ICL	13.8 ± 3.4
duplex 60-mer ICL[b]	23.1 ± 2.2

[a] Reactions were performed in 200 mM NaCl for 15-mers, 100 mM NaCl for 42-mers and 50 mM NaCl for 60-mer DNAs. [b] Data with 100 mM NaCl and 2 mM $MgCl_2$. [c] ND, data could not be fit.

electrophoresis which can result in smeared products. This likely explains the discrepancy in the results that we observed in Figure 2 with lower RPA binding to the cisplatin ICL duplex 15-mer (only a 7 base flanking region on either side of the ICL) compared with undamaged duplex 15-mer DNA.

RPA Binding Analysis Using Longer DNA Substrates. To further address the binding specificity of purified RPA and binding the flanking regions in the ICL DNA, longer length DNA substrates were utilized in EMSAs. Duplex 42-mer DNAs (undamaged, intra GXG and ICL) were incubated with increasing concentrations of RPA and resolved on native gels (Figure 4). As the DNA length increases and salt conditions (NaCl and $MgCl_2$) are increased to more stringent conditions, RPA binding to undamaged DNA is inhibited as a result of decreased denaturing activity (*19*). Divalent cations, especially Mg^{2+}, have been shown to stabilize the duplex DNA structure (*19, 32*). The binding of RPA to cisplatin intra specific DNA adducts is also inhibited, but not to the same extent as undamaged DNA. This is likely due to the structural distortion induced by the adduct which still enables localized RPA denaturation and results in preferential RPA DNA binding compared to undamaged DNA (*33*). In the EMSA, the degree of RPA binding to the undamaged DNA is much less than the intra (GXG) and ICL DNA substrates (Figure 4AB). In fact, increasing the DNA length from 15 to 42 bp results in better RPA binding to the ICL DNA substrate compared with the intra (GXG) DNA (compare Figure 4B with Figure 2B). Structurally, as the DNA length increases from 15 bp to 42 bp in the ICL DNA substrate (centrally located ICL), there is an increase of 14 bp (from 7 bp to 21 bp) that flanks the cross-link on either side. This flanking DNA is distorted by the cisplatin ICL and results in unstable DNA regions that RPA could bind to. EMSAs using duplex 60-mer DNAs support this finding and suggest as the DNA length further increases, and ultimately, the flanking DNA is lengthened, better RPA specificity occurs on the ICL DNA substrates (data not shown). This data demonstrates that RPA can specifically bind to cisplatin ICL damaged DNA and implicates the DNA flanking region of the ICL as an important feature for RPA binding.

Anisotopy on Longer DNA Substrates. The EMSAs give us qualitative analysis of the RPA binding and an initial comparison, but do not allow determination of the affinity (K_D) to ultimately compare binding to different DNA substrates. Thus, anisotropy experiments were conducted with

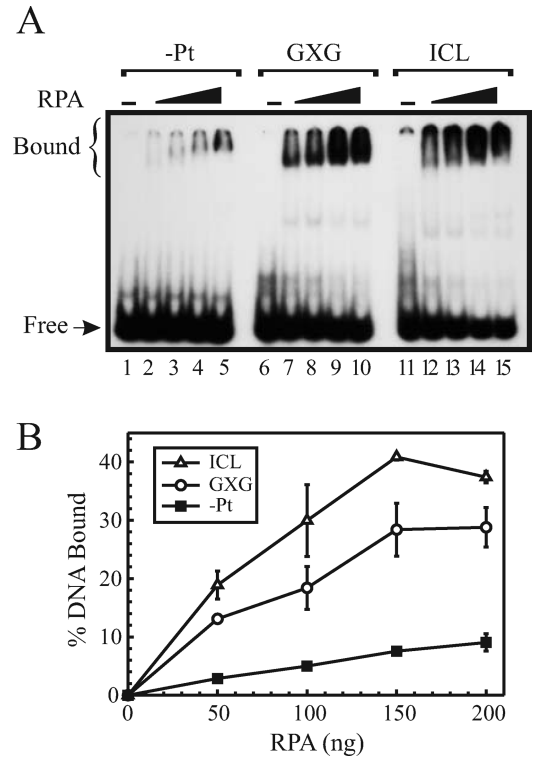

FIGURE 4: RPA preferentially binds duplex cisplatin ICL containing 42-mer DNA substrates. Duplex 42-mer DNA substrates, undamaged (-Pt), intra (GXG) or ICL were used in EMSAs to detect RPA DNA binding. In A, 50 fmol of each DNA substrate was incubated with increasing amounts of RPA (50−200 ng) in reactions containing 100 mM NaCl and 2 mM $MgCl_2$. The arrows indicate free DNA and bound (RPA-DNA) complexes. In B, the gels were quantified by PhosphorImager analysis, and each lane was plotted as a percentage of total DNA bound. The undamaged DNA is represented by squares, the intra GXG DNA by open circles and the ICL DNA by open triangles. Each point on the graph is the average of 3 individual experiments, and the error bars represent the standard deviation.

both the 42-mer DNAs (Figure 5A) and the 60-mer DNA substrates (Figure 5B) to quantify RPA affinities for the various substrates. The results are presented in Table 2. The salt conditions for each DNA substrate length had to be modified in order to analyze the undamaged DNA. Under higher salt conditions and the inclusion of $MgCl_2$, which stabilize the duplex DNA structure, it is difficult to accurately measure the affinity of RPA for the undamaged DNA as it takes a significant amount of RPA in the reactions to generate the plots to get near maximum r values. RPA binds duplex DNA via the denaturation of the DNA strands, and bulky DNA damage stimulates the ability of RPA to bind/denature duplex DNA oligonucleotides. For the 42-mers, 100 mM NaCl was used in the reactions, and for the 60-mer DNA substrates, 50 mM NaCl was used to generate the K_Ds for undamaged DNA. The results of the anisotropy demonstrate a substantial binding preference of RPA for the cisplatin ICL DNA (K_D is 8.4 nM and 13.8 nM for the 42 and 60-mer DNAs, respectively) compared with undamaged DNA (K_D is 1826 nM and 1390 nM for the 42 and 60-mer DNAs, respectively with the indicated salt concentrations). Under these conditions, there is also a slight RPA binding preference for the cisplatin ICL compared with the intra DNA substrates (2−4-fold difference in K_D).

Higher NaCl concentrations and the addition of 2 mM $MgCl_2$ into the reactions were used to create higher

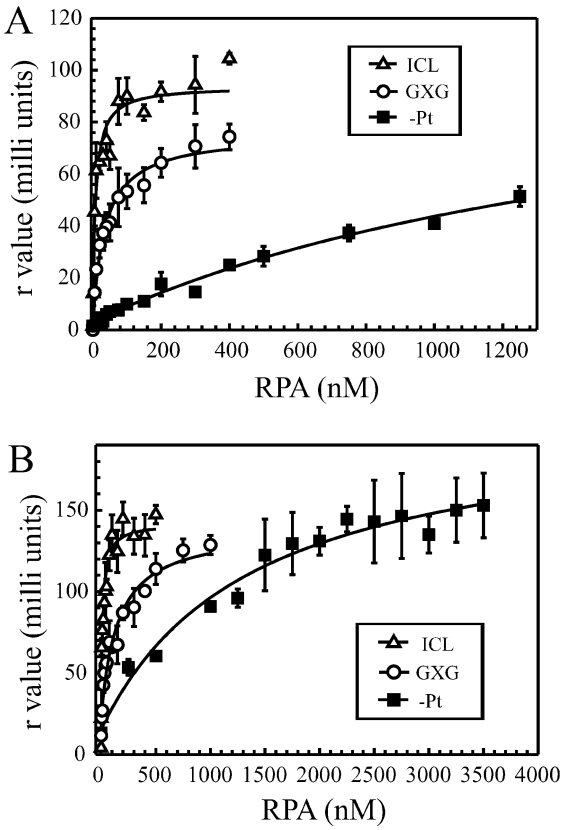

FIGURE 5: Anisotropy experiments reveal minimal change in RPA ICL DNA affinity with increasing salt concentrations. Duplex fluorescein labeled 42-mer and 60-mer DNA substrates were incubated with increasing RPA concentrations. In A, undamaged -Pt (squares), intra GXG (open circles) and ICL (open triangles) 42-mers were incubated with RPA in binding buffer containing 100 mM NaCl. In B, undamaged -Pt (squares), intra GXG (open circles) and ICL 60-mers were incubated with RPA in binding buffer containing 50 mM NaCl. Each data point represents the average of 6−9 experiments, and the error bars represent the standard deviation.

stringency binding conditions to compare the binding affinity of RPA to GXG and ICL DNA. As the salt concentrations are increased and $MgCl_2$ is added to the reactions (to stabilize the duplex structure of the 42-mer and 60-mer DNA and increase binding stringency), RPA binding to the cisplatin ICL DNA substrates is minimally affected, while the K_Ds for the undamaged and even the intra DNA substrates become difficult to determine (Figure 6 and Table 2). Even with increased RPA concentrations, the plot never reaches a maximum r value for the undamaged DNA substrates, making it impossible to calculate K_D based on these experiments (data not shown).

In the 42-mer analysis, as the binding conditions become more stringent with the addition of 2 mM $MgCl_2$, minimal effect is seen on RPA binding the ICL DNA (K_Ds of 8.4 nM compared with 13.8 nM, respectively). In the case of the 42-mer GXG, RPA's K_D is 36 nM and 81.7 nM, respectively under these conditions. The more stringent the conditions, the greater difference exists in RPA affinity between the cisplatin ICL and intra containing DNA substrates (4-fold versus a 6-fold difference in K_D values).

When comparing the 60-mer DNA substrates using 50 mM NaCl and 2 mM $MgCl_2$ in the reactions, there is about a 12-fold difference in K_D values for the ICL and intra DNA (data not shown). The increase in salt from 50 mM NaCl to

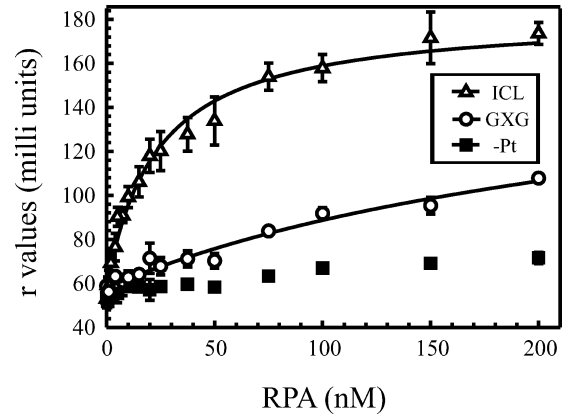

FIGURE 6: Increasing DNA binding stringency increases the RPA preference for cisplatin ICL DNA. Fluorescein labeled 60-mers were incubated with increasing RPA in DNA binding buffer containing 100 mM NaCl and 2 mM $MgCl_2$. Under these binding conditions, fitting the undamaged -Pt (squares) and the intra GXG DNA (open circles) was difficult and K_D values could not be obtained. Even with higher RPA concentrations, the r value would not reach a peak and fit to a hyberbolic equation for these substrates. The K_D for the cisplatin ICL (open triangles) is presented in Table 2. The data points represent 3−6 individual experiments, and the error bars represent the standard deviation.

100 mM NaCl along with 2 mM $MgCl_2$ minimally affects the ICL K_D (∼20 nM and ∼23 nM, respectively), while the K_D for the intra DNA increases from ∼225 nM (data not shown) to ∼1237 nM (Table 2). This results in a greater than 50-fold difference in K_D values between ICL and GXG 60-mer DNA substrates (∼23 nM compared with ∼1237 nM). As the DNA length is increased, the stability of the duplex DNA is higher with less effect of the DNA adduct on destabilization. When comparing the 42-mer and 60-mer DNA substrates, we observe greater RPA specificity to the ICL compared with the intra GXG on the longer 60-mer DNAs. This represents a moderate difference in affinity when compared with the ICL and undamaged DNA.

At high RPA concentrations (>400 nM), multiple RPA molecules can bind the ICL DNA substrates (both 42-mers and 60-mers) and the plots fit best with a 2-site protein binding mechanism where there is a K_{D1} and K_{D2} (data not shown). These higher protein concentrations likely induce a second RPA molecule binding to the DNA substrate, consistent with the higher r value observed under these conditions. Due to the cisplatin ICL DNA structure and RPA binding duplex damaged DNA via denaturation, one possibility for this observation is that, under high protein concentrations, one RPA trimer binds to each DNA side that flanks the ICL. Another possibility would be that one side of the duplex ICL DNA structure is denatured allowing one RPA on the top strand and one RPA molecule to the bottom complementary strand. The data for the K_{D1} in this case is very similar to the K_D values that we observe using lower RPA concentrations and fitting to a single one site protein binding mechanism. These data are all consistent with RPA playing a role in cisplatin ICL DNA recognition and repair initiation.

DISCUSSION

Many chemotherapeutic drugs target DNA and can form intra as well as ICL DNA adducts. The drugs that induce ICLs typically result in high cell sensitivity due to the

covalent link between the two DNA strands that forms an absolute block to the DNA replication machinery. Despite the importance in chemotherapy treatment, the repair of DNA ICLs is poorly understood. There appear to be several pathways and mechanisms that result in error free or error prone DNA repair (*23, 34*). The general belief is NER proteins, the recombination proteins and the translesion bypass polymerases all play some role in the processing and repair of ICLs. One model supports recruitment of DNA endonucleases, including XPF-ERCC1, to the damaged ICL DNA site, followed by dual incision flanking the ICL on one DNA strand (*35*). Flipping the damaged segment away from the duplex structure results in accessibility for a recombination event or polymerase bypass that likely involves REV1 and REV3 (*36, 37*). Following this step, a triplex DNA region would exist that is believed to be incised by the NER factors which would then be followed by DNA resynthesis and ligation.

How the different pathways and repair mechanisms initiate for ICLs has not been fully elucidated. It is still unclear if specific proteins can preferentially recognize the ICL damage and recruit endonucleases independent of S phase or if the majority of the repair is dependent on DNA replication and/or transcription coupled repair (*38, 39*). If an ICL is encountered during DNA replication, a DSB can arise as a result of replication fork collapse and cellular processing. Many of the ICL agents induce DSBs, specifically in S phase, and are generally viewed as generating the same lesion and resulting in the same DNA repair pathways (*39*). There is evidence, however, in the literature that argues that certain ICL agents, like cisplatin, generate fewer DSBs, which suggests that other DNA repair pathways would prevail prior to replication fork collapse (*40*). This also suggests that unique structural features of each ICL agent may dictate which repair pathway responds and, ultimately, control how proteins recognize and initiate the ICL repair process. The cisplatin ICLs induce a unique structural distortion that bends and unwinds the DNA as well as induces extrahelical flipping of cytosine residues that flank the cross-linked guanines (*41*). These structural features are a unique feature of cisplatin and are not displayed in mitomycin C and psoralen ICL structures (*42, 43*).

It has previously been shown for psoralen ICLs that RPA is required for the initial incision and polymerase resynthesis (*26*). In this report, we have demonstrated that RPA can bind cisplatin induced ICLs and displays a significantly higher affinity compared with undamaged DNA and a moderately higher affinity compared with intra containing DNA substrates. Increasing the DNA length and the salt concentrations to stabilize the duplex DNA results in a minimal effect on the affinity of RPA for the cisplatin ICL, whereas significant decreases in the affinity for undamaged is observed. The specificity of RPA binding to the ICL DNA compared with the intra GXG can also be made greater by increasing the stringency in the binding reactions and increasing the DNA length. These results are consistent with RPA playing a role in cisplatin ICL DNA recognition and repair initiation.

RPA binds duplex damaged DNA via its ability to denature the DNA and disrupt the hydrogen bonds between complementary bases (*11, 19*). For bulky type DNA damage like the cisplatin intrastrand GXG adducts, shorter DNA substrates *in vitro* are bound with fairly high affinity by RPA (*21*). The DNA adduct bends and distorts the DNA structure, ultimately disrupting the hydrogen bonds and enabling RPA to denature the strands and bind to the undamaged ssDNA that is generated. The bulky cisplatin adducts on ssDNA have been shown to inhibit RPA binding (*21*). As the DNA length increases and the stability of the duplex DNA is enhanced, the binding affinity of RPA to cisplatin intra GXG substrates is reduced (Table 2). As mentioned above, the cisplatin ICL generates a unique type of DNA structural distortion and forms a covalent link between two guanines on opposite strands in DNA. The covalent link prevents strand denaturation at the localized cross-links, but DNA bending and distortion is evident on both sides of the cross-link (*30*). Our data suggests that RPA binding to the cisplatin ICL and damage specificity (compared with undamaged and intrastrand DNA) is greater as the DNA length increases. One possible mechanism for RPA binding cisplatin ICL DNA is via structural distortions in the DNA duplex that flanks the cross-link. On shorter DNA duplexes (like 15-mers), the flanking DNA is only about 7 bp in length. RPA has been shown to bind with low affinity to ssDNA substrates shorter than 12 bases in length (*2*). In our reactions, as the DNA length increases from 15 bp to 42 bp in length, we observe better RPA−ICL DNA binding and the specificity is increased. This would result in the flanking DNA going from about 7 bases to 21 bp, which has been shown to result in greater RPA binding to ssDNA (*2*). The increase to 60-mer DNAs would generate flanking DNA lengths of 30 bp, the DNA length that supports all DBD contact, is optimal for ssDNA binding and is the DNA length that is occluded by RPA (*2*). Having two sites of DNA distortion within the cisplatin ICL, as opposed to one in the bulky intrastrand adducts, likely has a positive effect on the affinity of RPA for the ICL and may play a role in the specificity for the ICL.

This work provides insight into protein ICL recognition and why certain repair pathways may prevail for the different ICL inducing agents. It will be interesting to see if RPA can provide a scaffold and recruit XPF-ERCC1 to the cisplatin ICL damaged site to stimulate DNA incision and also to see if RPA binds in a unique polarity or strand specific manner, as has been seen for NER (*12*). How the other NER factors like XPC-hHR23B influence RPA cisplatin ICL binding and subsequent protein recruitment and processing will add significant input to the ICL repair mechanisms and how these processes are regulated.

ACKNOWLEDGMENT

We would like to thank Jeremy Keirsey and Kristen Sullivan for helping with some experimental aspects of this manuscript. We would also like to thank Anbarasi Kothandapani for critical reading of the manuscript.

SUPPORTING INFORMATION AVAILABLE

DNA affinity columns were prepared using calf thymus DNA. The DNA was sonicated to produce DNA fragments 400−800 bp in length and either left untreated (-Pt), treated with a low cisplatin concentration for intra DNA adducts or treated at high cisplatin levels to induce ICL DNA. HeLa crude protein extracts were passed over each column, followed by washing and then bound protein was eluted with

high salt buffer. The results indicated that RPA was preferentially retained on the cisplatin ICL and intra DNA columns compared with undamaged DNA. Different salt conditions and wash steps were utilized to assess the RPA binding retention on the ICL and intra DNA columns. The data indicated similar binding and dissociation of RPA from the intra and ICL columns (Figure S1). This data is consistent with RPA having an affinity for cisplatin ICLs. This material is available free of charge via the Internet at http://pubs.acs.org.

REFERENCES

1. Wold, M. S., and Kelly, T. (1988) Purification and characterization of replication protein-A, a cellular protein required for in vitro Replication Of Simian Virus-40 DNA. *Proc. Natl. Acad. Sci. U.S.A. 85*, 2523–2527.
2. Wold, M. S. (1997) Replication protein A: A heterotrimeric, single-stranded DNA- binding protein required for eukaryotic DNA metabolism. *Annu. Rev. Biochem. 66*, 61–92.
3. Kenny, M. K., Schlegel, U., Furneaux, H., and Hurwitz, J. (1990) The role of human single-stranded-DNA binding-protein and its Individual subunits in simian virus-40 DNA-replication. *J. Biol. Chem. 265*, 769–7700.
4. Kenny, M. K., Lee, S. H., and Hurwitz, J. (1989) Multiple functions of human single-stranded-DNA binding-protein in simian virus-40 DNA-replication - single-strand stabilization and stimulation of DNA polymerase-alpha and polymerase-delta. *Proc. Natl. Acad. Sci. U.S.A. 86*, 9757–9761.
5. Coverley, D., Kenny, M. K., Munn, M., Rupp, W. D., lane, D. P., and Wood, R. D. (1991) Requirement for the replication protein SSB in human DNA excision repair. *Nature 349*, 538–541.
6. Ramilo, C., Gu, L. Y., Guo, S. L., Zhang, X. P., Patrick, S. M., Turchi, J. J., and Li, G. M. (2002) Partial reconstitution of human DNA mismatch repair in vitro: characterization of the role of human replication protein A. *Mol. Cell. Biol. 22*, 2037–2046.
7. Park, M. S., Ludwig, D. L., Stigger, E., and Lee, S. H. (1996) Physical interaction between human RAD52 and RPA is required for homologous recombination in mammalian cells. *J. Biol. Chem. 271*, 18996–19000.
8. Matsunaga, T., Park, C. H., Bessho, T., Mu, D., and Sancar, A. (1996) Replication protein A confers structure-specific endonuclease activities to the XPF-ERCC1 and XPG subunits of human DNA repair excision nucleases. *J. Biol. Chem. 271*, 11047–11050.
9. Braun, K., Lao, Y., He, Z., Ingles, C., and Wold, M. (1997) Role of protein-protein interactions in the function of replication protein A (RPA): RPA modulates the activity of DNA polymerase alpha by multiple mechanisms. *Biochemistry 36*, 8443–8454.
10. Wakasugi, M., and Sancar, A. (1999) Order of assembly of human DNA repair excision nuclease. *J. Biol. Chem. 274*, 18759–18768.
11. Missura, M., Buterin, T., Hindges, R., Hubscher, U., Kasparkova, J., Brabec, V., and Naegeli, H. (2001) Double-check probing of DNA bending and unwinding by XPA-RPA: an architectural function in DNA repair. *EMBO J. 20*, 3554–3564.
12. de Laat, W. L., Appeldoorn, E., Sugasawa, K., Weterings, E., Jaspers, N. G. J., and Hoeijmakers, J. H. J. (1998) DNA-binding polarity of human replication protein A positions nucleases in nucleotide excision repair. *Genes Dev. 12*, 2598–2609.
13. Bochkarev, A., Pfuetzner, R. A., Edwards, A. M., and Frappier, L. (1997) Structure of the single-stranded-DNA-binding domain of replication protein A bound to DNA. *Nature 385*, 176–181.
14. Brill, S., and Bastin-Shanower, S. (1998) Identification and characterization of the fourth single- stranded-DNA binding domain of replication protein A. *Mol. Cell. Biol. 18*, 7225–7234.
15. Gomes, X. V., and Wold, M. S. (1996) Functional domains of the 70-kilodalton subunit of human replication protein A. *Biochemistry 35*, 10558–10568.
16. Jacobs, D., Lipton, A., Isern, N., Daughdrill, G., Lowry, D., Gomes, X., and Wold, M. (1999) Human replication protein A: global fold of the N-terminal RPA- 70 domain reveals a basic cleft and flexible C-terminal linker. *J. Biomol. NMR 14*, 321–331.
17. Bochkarev, A., Bochkareva, E., Frappier, L., and Edwards, A. (1999) The crystal structure of the complex of replication protein A subunits RPA32 and RPA14 reveals a mechanism for single-stranded DNA binding. *EMBO J. 18*, 4498–4504.
18. Bochkareva, E., Korolev, S., Lees-Miller, S. P., and Bochkarev, A. (2002) Structure of the RPA trimerization core and its role in the multistep DNA-binding mechanism of RPA. *EMBO J. 21*, 1855–1863.
19. Patrick, S. M., and Turchi, J. J. (1998) Human replication protein a preferentially binds cisplatin- damaged duplex DNA in vitro. *Biochemistry 37*, 8808–8815.
20. Patrick, S. M., and Turchi, J. J. (1999) Replication protein A (RPA) binding to duplex cisplatin-damaged DNA is mediated through the generation of single-stranded DNA. *J. Biol. Chem. 274*, 14972–14978.
21. Patrick, S. M., and Turchi, J. J. (2001) Stopped-flow kinetic analysis of replication protein A-binding DNA - Damage recognition and affinity for single-stranded DNA reveal differential contributions of k(on) and k(off) rate constants. *J. Biol. Chem. 276*, 22630–22637.
22. Eastman, A. (1987) The formation, isolation and characterization of DNA adducts produced by anticancer platinum complexes [Review] [57 refs]. *Pharmacol. Ther. 34*, 155–166.
23. Wang, X., Peterson, C. A., Zheng, H. Y., Nairn, R. S., Legerski, R. J., and Li, L. (2001) Involvement of nucleotide excision repair in a recombination- independent and error-prone pathway of DNA interstrand cross- link repair. *Mol. Cell. Biol. 21*, 713–720.
24. Zheng, H. Y., Wang, X., Warren, A. J., Legerski, R. J., Nairn, R. S., Hamilton, J. W., and Li, L. (2003) Nucleotide excision repair- and polymerase eta-mediated error- prone removal of mitomycin C interstrand cross-links. *Mol. Cell. Biol. 23*, 754–761.
25. Wu, Q., Christensen, L. A., Legerski, R. J., and Vasquez, K. M. (2005) Mismatch repair participates in error-free processing of DNA interstrand crosslinks in human cells. *EMBO Rep. 6*, 551–556.
26. Li, L., Peterson, C. A., Zhang, X. S., and Legerski, R. J. (2000) Requirement for PCNA and RPA in interstrand crosslink-induced DNA synthesis. *Nucleic Acids Res. 28*, 1424–1427.
27. Vasquez, K. M., Christensen, J., Li, L., Finch, R. A., and Glazer, P. M. (2002) Human XPA and RPA DNA repair proteins participate in specific recognition of triplex-induced helical distortions. *Proc. Natl. Acad. Sci. U.S.A. 99*, 5848–5853.
28. Turchi, J. J., Patrick, S. M., and Henkels, K. M. (1997) Mechanism of DNA-dependent protein kinase inhibition by cis- diamminedichloroplatinum(II)-damaged DNA. *Biochemistry 36*, 7586–7593.
29. Hey, T., Lipps, G., and Krauss, G. (2001) Binding of XPA and RPA to damaged DNA investigated by fluorescence anisotrophy. *Biochemistry 40*, 2901–2910.
30. Lemaire, M. A., Schwartz, A., Rahmouni, A. R., and Leng, M. (1991) Interstrand cross-links are preferentially formed at the d(GC) sites in the reaction between cis-diamminedichloroplatinum(II) and DNA. *Proc. Natl. Acad. Sci. U.S.A. 88*, 1982–1985.
31. Patrick, S. M., Oakley, G. G., Dixon, K., and Turchi, J. J. (2005) DNA damage induced hyperphosphorylation of replication protein A. 2. Characterization of DNA binding activity, protein interactions, and activity in DNA replication and repair. *Biochemistry 44*, 8438–8448.
32. Xu, Y., and Bremer, H. (1997) Winding of the DNA helix by divalent metal ions. *Nucleic Acids Res. 25*, 4067–4071.
33. Poklar, N., Pilch, D. S., Lippard, S. J., Redding, E. A., Dunham, S. U., and Breslauer, K. J. (1996) Influence of cisplatin intrastrand crosslinking on the conformation, thermal stability, and energetics of a 20-mer DNA duplex. *Proc. Natl. Acad. Sci. U.S.A. 93*, 7606–7611.
34. Dronkert, M. L. G., and Kanaar, R. (2001) Repair of DNA interstrand cross-links. *Mutat. Res.-DNA Repair 486*, 217–247.
35. Kuraoka, I., Kobertz, W. R., Ariza, R. R., Biggerstaff, M., Essigmann, J. M., and Wood, R. D. (2000) Repair of an interstrand DNA cross-link initiated by ERCC1-XPF repair/recombination nuclease. *J. Biol. Chem. 275*, 26632–26636.
36. Zhang, N. X., Liu, X. P., Li, L., and Legerski, R. (2007) Double-strand breaks induce homologous recombinational repair of interstrand cross-links via cooperation of MSH2, ERCC1-XPF, REV3, and the Fanconi anemia pathway. *DNA Repair 6*, 1670–1678.
37. Shen, X., Jun, S., O'Neal, L. E., Sonoda, E., Bemark, M., Sale, J. E., and Li, L. (2006) REV3 and REV1 play major roles in recombination-independent repair of DNA interstrand cross-links mediated by monoubiquitinated proliferating cell nuclear antigen (PCNA). *J. Biol. Chem. 281*, 13869–13872.
38. Akkari, Y. M. N., Bateman, R. L., Reifsteck, C. A., Olson, S. B., and Grompe, M. (2000) DNA replication is required to elicit cellular responses to psoralen-induced DNA interstrand cross-links. *Mol. Cell. Biol. 20*, 8283–8289.

39. Bessho, T. (2003) Induction of DNA replication-mediated double strand breaks by psoralen DNA interstrand cross-links. *J. Biol. Chem. 278*, 5250–5254.
40. De Silva, I. U., McHugh, P. J., Clingen, P. H., and Hartley, J. A. (2002) Defects in interstrand cross-link uncoupling do not account for the extreme sensitivity of ERCC1 and XPF cells to cisplatin. *Nucleic Acids Res. 30*, 3848–3856.
41. Huang, H. F., Zhu, L. M., Reid, B. R., Drobny, G. P., and Hopkins, P. B. (1995) Solution structure of a cisplatin-induced DNA interstrand cross-link. *Science 270*, 1842–1845.
42. Kumaresan, K. R., Ramaswamy, M., and Yeung, A. T. (1992) Structure of the DNA interstrand cross-link of 4,5′,8-trimethylpsoralen. *Biochemistry 31*, 6774–6783.
43. Fagan, P. A., Spielmann, H. P., Sigurdsson, S. T., Rink, S. M., Hopkins, P. B., and Wemmer, D. E. (1996) An NMR study of [d(CGCGAATTCGCG)](2) containing an interstrand cross-link derived from a distamycin-pyrrole conjugate. *Nucleic Acids Res. 24*, 1566–1573.

BI800460D